


SYNTHESIS AND CHARACTERIZATION OF Al-PILLARED BENTONITE FOR REMEDIATION OF CHLORINATED PESTICIDE-CONTAMINATED WATER



MOHAMED S. BASIONY¹, SELEEM E. GABER¹, HOSNY IBRAHIM², AND EMAD A. ELSHEHY³ * 

¹Central Laboratory for Environmental Quality Monitoring, National Water Research Center, El-Kanater, Kalyubeya, Egypt

²Chemistry Department, Faculty of Science, Cairo University, Giza, Egypt

³Nuclear Materials Authority, P.O. Box 530, El-Maadi, Cairo, Egypt

Abstract—The removal of pesticide contaminants from water is a key priority in environmental remediation, and requires intensive effort; this necessitates modification of the properties of pillared clays (PILCs) such as porosity, pore-volume, surface area, and synthesis methods. The purpose of the present study was to test the ability of Al-pillared bentonite (Al-PILB), using $[Al_{13}O_4(OH)_{24}(H_2O)_{12}]^{7+}$ and $[Al_{30}O_8(OH)_{56}(H_2O)_{24}]^{18+}$ (keggin cations, Al_{13} and Al_{30}) as pillars, to adsorb chlorinated pesticides from contaminated water. In order to maximize intercalation and uniformity of layer stacking, various ratios of the nitrate forms of the synthesized keggin cations were intercalated into the natural bentonite (BT). The synthesized materials (Al-PILBs) were characterized by various techniques, including X-ray diffraction (XRD), scanning electron microscopy (SEM), energy dispersive X-ray analysis (EDX), Fourier-transform infrared (FTIR) spectroscopy, UV-Vis spectroscopy, and N_2 adsorption-desorption measurements. Increases in basal spacing, surface area, and pore volume were observed. The adsorption capacity of the Al-PILBs for 17 types of chlorinated pesticides from contaminated water was better than using the BT alone, e.g. for heptachlor epoxide, dieldrin, and endrin at natural pH, the maximum adsorptions obtained at equilibrium solution concentrations of 16, 20, and 20 $\mu\text{g/L}$, respectively, were 59.2, 59.15, and 60 $\mu\text{g/g}$, whereas corresponding values using pristine BT were 34.68, 39.45, and 38.9, respectively. The data were best described by the Freundlich adsorption model.

Keywords—Bentonite · Intercalation · Keggin cations · Pillared clay · Porous materials

INTRODUCTION

The increasing use of pesticides is a great global challenge due to their detrimental effect on surface water, air, soil, and living organisms. Thus, the use of pesticides has reduced the quantity and quality of global water resources. They exhibit harmful impacts and cause severe health problems, such as cancers, mutations, immuno-toxicity, paralysis, tonic clonic convulsions, and alterations to nervous and reproductive systems (El-Said et al. 2018). Most chlorinated pesticides such as endrin, dieldrin, and heptachlor epoxide are non-degradable; hence, they accumulate in human blood up to the warning levels established by international agencies (WHO 1989; IPCS 1992; WHO 2004). Several studies have focused on the removal of pesticides from water. One traditional approach for pesticide removal is based on decomposition into smaller or insoluble molecules that precipitate at the bottom of the water reservoir or stream (Morales-Pérez et al. 2015). Decomposition of pesticides, however, may produce toxic byproducts which could represent a greater risk to the environment and human health than the parent molecule (Hladik et al. 2005). Diversified methods have been reported for sequestration of pesticides from the aquatic environment such as oxidation, adsorption, solvent extraction, biodegradation, ozonation, and adsorption. Among the diversified methods, adsorption is still an efficient, simple, and promising fundamental technique for water decontamination (Bonilla-Petriciolet et al. 2017), and various adsorbents have been used for this purpose (De Wilde et al. 2009).

Nowadays, designed and functionalized porous materials play an essential role in developing active surfaces which operate as adsorbents and catalysts. In order to achieve a precise molecular selectivity in the removal of organic pollutants, much effort has been made to optimize the shape and size of pores. Pillared clays (PILCs) are among the most interesting porous materials due to their permanent and engineered porosity and large specific surface area (Zhu et al. 2017). Bentonite (BT) is of particular interest and is one of the most promising PILCs for applications that require high-efficiency adsorbents or catalysts. Bentonites are classified into three types: Na-bentonite, Ca-bentonite, and mixed Na/Ca-bentonite (Şans et al. 2017). The Na-bentonites are well dispersed, viscous, have a high swelling index, and greater electrical conductivity than the Ca-bentonites. Such forms of BT are a competitive alternative to activated carbon and zeolite because of their wide availability, low price, and the acidic nature of their surfaces, which enrich their chemical reactivity (Vicente and Lambert 2003; Aznárez et al. 2015; Cheira et al. 2019). The pores and surfaces of BT can be tailored further for specific purposes by exchanging the Na or Ca with large organic or inorganic cations which impart a change in pore shape and which in turn affects the selectivity toward specific molecules (Yuan et al. 2006). The interlayer spaces of these layered materials can also be stabilized against swelling and expansion by intercalating rigid pillars which further define the pore structure and nature of surfaces and make them even more suitable for selectively accommodating certain molecules (Okada et al. 2014).

Earlier attempts to modify PILCs were created by intercalating organic cations, such as tetraalkylammonium cations, and releasing the inorganic cations from the clay interlayer

* E-mail address of corresponding author: eelshehy@yahoo.com
DOI: 10.1007/s42860-020-00072-y

spaces through cation exchange (Barrer 1986). This concept was extended further to include other layered minerals and compounds with the ability to exfoliate fully the clay minerals to form individual, atomically thin layers (Abdelkader et al. 2015). Despite their versatility and greater basal spacing, intercalation by organic cations imposed certain limitations such as low thermal stability (Aznárez et al. 2015). PILCs can also be created using inorganic polyoxycations to form the pillars. With a suitable choice of polyoxycation, the pillared interlayers can be kept stable at higher temperatures (Ming-li et al. 2002). The preparation of inorganic PILCs involves four steps: (1) ensuring that the clay is in the sodium form 'Na-montmorillonite'; (2) formulation of the target pillaring agent; (3) intercalation by cation exchange; and (4) calcination to obtain the final stable form of the composite (Cool and Vansant 1998).

Many Al oligomers have been prepared through dilute hydrolytic polymeric Al solution (HPA) (Del Riego et al. 1994; Schoonheydt et al. 1994; Kumararaja et al. 2017). The formation of target Al oligomers is achieved by controlling: (1) the molar ratio of Al to OH; (2) the initial Al^{3+} concentration in solution; (3) the rate of base addition; (4) the hydrolyzed solution temperature; and (5) the aging time of the hydrolyzed solution (Cool and Vansant, 1998). The transformation of $[\text{Al}_{13}\text{O}_4(\text{OH})_{24}(\text{H}_2\text{O})_{12}]^{7+}$ (Al_{13}) into $[\text{Al}_{30}\text{O}_8(\text{OH})_{56}(\text{H}_2\text{O})_{24}]^{18+}$ (Al_{30}) oligomers was reported by Rowsell and Nazar (2000). The intercalation process focused on preparing concentrated suspensions from the pillaring agents (Chen et al. 2007). Schoonheydt and Leeman (1992) prepared Al-PILBs through the addition of the clay to the Al polycation solution. Aouad et al. (2006) developed a method for synthesis of Al-PILBs that minimizes the amount of water used, allowing for its extension to the industrial scale. Bentonite with mixed pillars, achieved using the concentration method, offers numerous potential applications of environmental interest, due to the possibility of introducing a large polyoxycation with favorable characteristics.

The objective of the current study was to design and synthesize aluminum pillared bentonites (Al-PILBs) with large surface areas and pore volumes and controllable pore size through the concentration method, beginning with the nitrate form of Al_{13} and Al_{30} Keggin cations with various molar ratios; and to investigate the possibility of using the Al-PILBs synthesized for the removal of chlorinated pesticides from aqueous solution.

MATERIALS AND METHODS

Materials

All chemicals used in this study were of analytical grade and deployed without further purification. The chemicals used were aluminum chloride hexahydrate ($\text{AlCl}_3 \cdot 6\text{H}_2\text{O}$), ammonium chloride (NH_4Cl), and ammonium acetate ($\text{CH}_3\text{COONH}_4$) obtained from LOBA Chemie (Mumbai, India); sodium hydroxide (NaOH) pellets from Honeywell (Neuss, Germany); and silver nitrate (AgNO_3), barium nitrate ($\text{Ba}(\text{NO}_3)_2$), anhydrous sodium sulfate (Na_2SO_4), Ferron (8-hydroxy-7-iodo-5-quinolinesulfonic acid ($\text{C}_9\text{H}_6\text{INO}_4\text{S}$), 1,10-phenanthroline

($\text{C}_{12}\text{H}_8\text{N}_2$), and hydroxylamine hydrochloride ($\text{NH}_2\text{OH} \cdot \text{HCl}$) from Sigma-Aldrich (Taufkirchen, Germany). The bentonite (Na form), consisting mostly of montmorillonite (assay >95% with some minor impurities of quartz and Fe_2O_3), was obtained from Egypt Bentonite & Derivatives Company (New Borg El Arab city, Alexandria, Egypt). Standard chlorinated pesticide solutions (1000 mg/L) containing 17 types of pesticides (α -BHC, β -BHC, σ -BHC, heptachlor, aldrin, heptachlor epoxide, endosulfane 1, dieldrin, DDE, endrin, endosulfan 2, DDD, endrin aldehyde, endosulfan sulfate, DDT, methoxychlor, and γ -BHC) were acquired from AccuStandard (New Haven, Connecticut, USA). Deionized water (DIW) used in all experimental steps had an electric conductivity of 0.7 $\mu\text{S}/\text{cm}$.

Synthesis of Al_{13} and Al_{30} Sulfate

Aluminum oligomers of Al_{13} and Al_{30} sulfate were prepared using the usual synthesis procedures described by Aouad et al. (2005). In this method, 0.6 M NaOH was added dropwise to a 500 mL round flask containing 1 M $\text{AlCl}_3 \cdot 6\text{H}_2\text{O}$ with a flow rate of 4 mL/min while stirring at 80°C. The temperature of the solution was then increased to 95°C with continuous stirring for various intervals (40 min for Al_{13} and 12 h for Al_{30}). The solution mixtures obtained became transparent, were left to cool gradually, and were then kept for 5 days at room temperature; the pH was adjusted to 4.22 and 4.53 for Al_{13} and Al_{30} solutions, respectively. Then, 0.5 M Na_2SO_4 solution was added to each of the Al_{13} and Al_{30} solutions to obtain a $\text{SO}_4^{2-}/\text{Al}^{3+}$ ratio of 0.33 at which white colloidal suspensions of Al_{13} and Al_{30} sulfate were formed after stirring for an additional 10 min. The colloidal suspensions produced were kept with the mother liquor for 72 h at 25°C. The obtained precipitate of Al_{13} and Al_{30} sulfate oligomers was collected by filtration and washed several times with DIW then dried in air for 24 h to obtain Al_{13} and Al_{30} nitrate crystals (Zhou et al. 2006).

Synthesis of Al_{13} and Al_{30} Nitrates

The Al_{13} and Al_{30} sulfates prepared were used as precursors for the synthesis of Al_{13} and Al_{30} nitrates, according to the method proposed by Furrer et al. (1992). A 3.6 g portion of Al_{13} sulfate or 3.26 g of Al_{30} sulfate was dissolved in 800 mL of 1.0×10^{-2} M or 1.15×10^{-2} M of $\text{Ba}(\text{NO}_3)_2$, respectively, under vigorous stirring for 5 h. The products obtained were filtered out using 0.1 μm filter paper, and the filtrate was then crystallized in an oven at 60°C to obtain Al_{13} and Al_{30} nitrate crystals (Aouad et al. 2006).

Synthesis of Al-PILBs

1 g of BT with a grain size of ~20 μm was ground using a porcelain mortar with 0.17 g of Al_{13} nitrate or 0.15 g of Al_{30} nitrate, or a mixture of the two in a 1:1, 2:1, or 1:2 ratio; the mixture was then transferred to a conical flask containing 7.5 mL of DIW, stirred for 60 min, and then covered and left to stand overnight. The polyoxycation/BT ratio used in the synthesis of all Al-PILBs materials was 0.806 meq Al/g BT. The products obtained were filtered off using 0.45 μm Millipore filter paper, dried at 120°C for 12 h, and then calcined at 300°C

for 3 h. The synthesized materials were labeled BT, BT-Al₃₀, BT-Al₁₃/Al₃₀, BT-Al₁₃/2Al₃₀, or BT-2Al₁₃/Al₃₀.

Characterization Techniques

Estimation of the raw BT sample constituents (wt.%) was performed using X-ray fluorescence (Shimadzu 2400, Kyoto, Japan). The morphologies of Al-PILBs were characterized by field-emission scanning electron microscopy (FESEM, QUANTA FEG250, Eindhoven, The Netherlands). FTIR spectra were obtained using an advanced FTIR spectrometer (Shimadzu IRTracer-100, Kyoto, Japan). X-ray diffraction (XRD) patterns were measured on a Philips X-ray diffractometer model PW/103 (Eindhoven, The Netherlands). Surface area, pore volume, and pore-size distribution were measured by the N₂ adsorption/desorption technique using a QuantaChrome (Boynton Beach, Florida, USA) Nova touch LX2 surface area and pore size analyzer. The various species of Al in HPA solutions were quantified by the Ferron colorimetric method (Chen et al., 2007) using a UV-Vis spectrophotometer (HACH, DR-3900, Colorado, USA). Finally, pesticide concentrations were determined using gas chromatography-mass spectrometry (GC-MS, Agilent Technologies, Santa Clara, California, USA), model 7890A GC System.

Removal of Chlorinated Pesticides from Water using Al-PILBs

A mixture of the 17 types of chlorinated pesticides mentioned above (1000 mg/L diluted in a mixture of n-hexane/water (1:20)) was used in this study. The pesticide mixture comprises the most abundant pesticides in environmental samples. Initially, 1 g of each Al-PILB material (BT-Al₃₀, BT-Al₁₃/Al₃₀, BT-Al₁₃/2Al₃₀, BT-2Al₁₃/Al₃₀, or BT) was dried at 120°C for 3 h to remove physisorbed water. Then, a series of batch experiments was performed to examine the applicability of Al-PILB materials to pesticide removal from a dilute solution. In a typical adsorption experiment, the Al-PILB (25 mg) was mixed with 25 mL of an aqueous solution containing pesticide in the range 200–300 µg/L and adjusted to the appropriate pH at the natural value (5.8). The mixture was shaken using an orbital shaker in a temperature-controlled water bath at 25°C for 5 h at a constant agitation speed of 400 rpm. After equilibration, the Al-PILB was filtered using a 25 mm Whatman filter paper and the filtrate was used for adsorption assessment by analyzing the pesticide concentrations using GC-MS. The removal efficiency (R_E) and adsorption capacity (q_e) of Al-PILBs were calculated using the following equations (Eqs 1 and 2) (El-Said et al. 2018; Hamza et al. 2019):

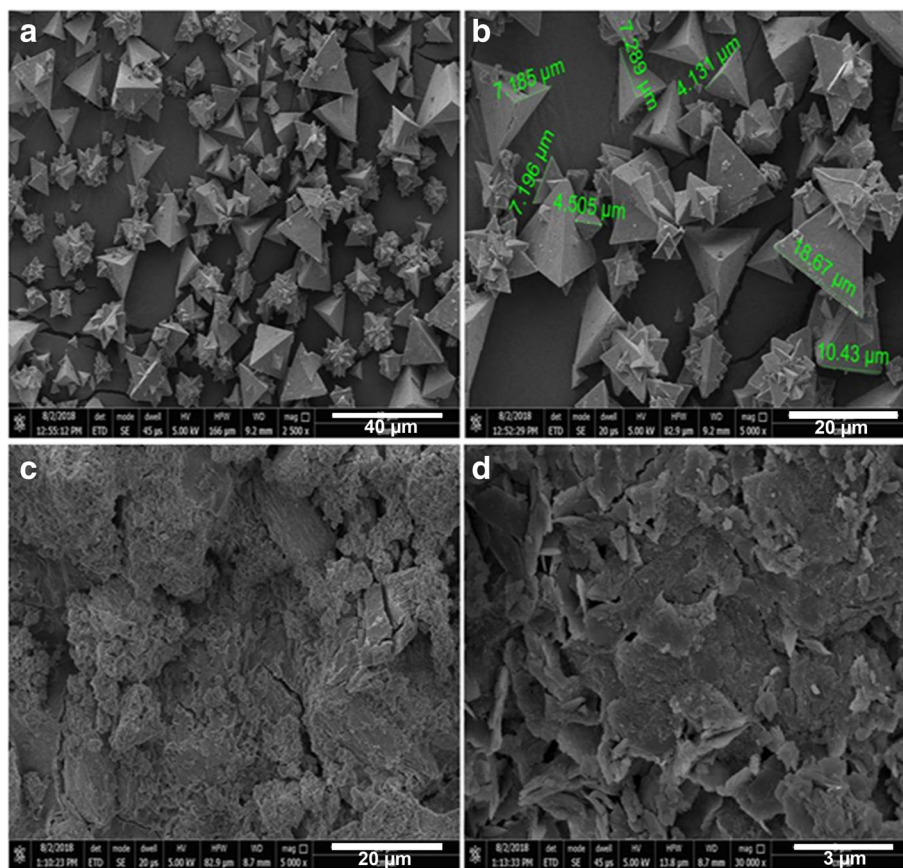


Fig. 1. Representative SEM images for the synthesized Al₁₃ a, b and Al₃₀ sulfate c, d at various magnifications

$$R_E \% = \frac{C_i - C_e}{C_i} \times 100 \quad (1)$$

$$q_e = \frac{C_i - C_e}{W} \times V \quad (2)$$

where C_i and C_e are the initial and equilibrium concentrations of the pesticide ($\mu\text{g/L}$), respectively; V is the volume of solution (L); and W is the weight of Al-PILB material (g).

RESULTS AND DISCUSSION

Materials Characterization

The synthesized Keggin cations of Al_{13} and Al_{30} were prepared in the sulfate form then converted to the nitrate form to give uniformly intercalated and stacked layers (Aouad et al. 2006). In spite of the large size of the Al_{30} polyoxycations, their high charge stabilizes their accommodation inside BT layers better

than Al_{13} cations. Such systematic changes led to two significant characteristics of the Al_{30} polyoxycations: (1) the particulate size development and high charge lead to appreciable changes in interlayer spacing; and (2) the hydrolysis rate and species stability might provide a driving force for changing the morphology and structure of the Keggin cation formed (Lin et al. 2008).

Chemical Composition

In the present study, the bentonite sample contained mainly montmorillonite accompanied by some impurities of kaolinite, illite, and quartz. The bentonite was used without thermal or chemical treatment. The main chemical composition (expressed as oxides) given by the XRF analysis was SiO_2 (55.9%), Al_2O_3 (16.87%), Fe_2O_3 (9.07%), MgO (0.88%), CaO (2.39%), K_2O (1.47%), TiO_2 (1.06%), and Na_2O (3.67%).

SEM Analysis

The surface micrographs of poly-aluminum species of Al_{13} and Al_{30} Keggin were elucidated using SEM analysis. The

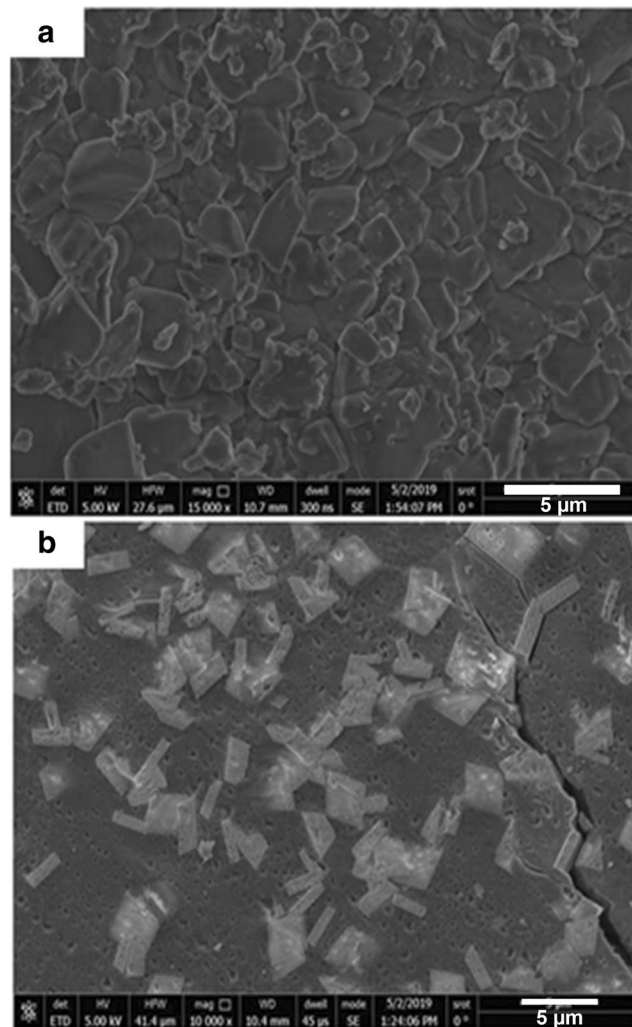


Fig. 2. Representative SEM images for the synthesized **a** Al_{13} - and **b** Al_{30} -nitrate

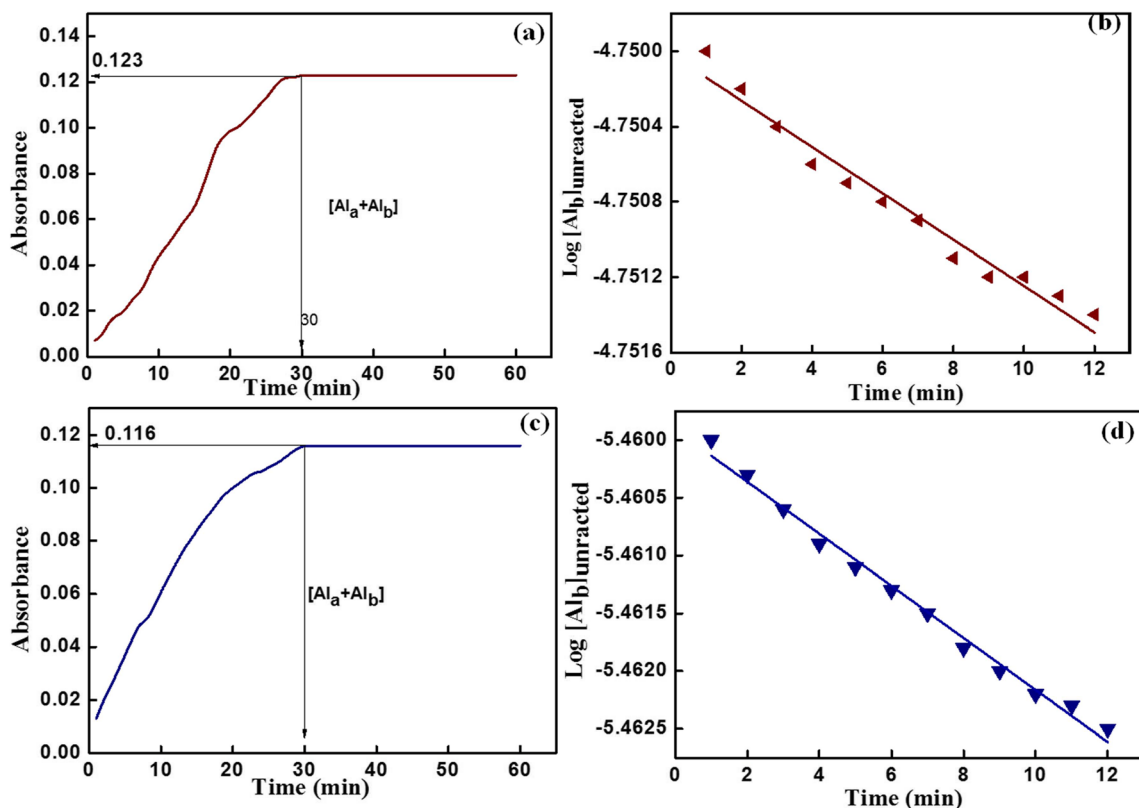


Fig. 3. Al-Ferron reaction kinetics (at $\lambda_{\max} = 370$ nm) for the reaction of **a** Al_{13} and **b** Al_{30} with Ferron and $\log [\text{Al}_b]$ unreacted Al_{13} and Al_{30} solutions as a function of time **c**, **d**, respectively

crystals of Al_{13} and Al_{30} sulfate formed showed different morphologies depending on the aging time (Wang and Muhammed 1999). The SEM images for Al_{13} associated with the sulfate anions at various magnifications (Fig. 1a,b) revealed tetrahedral morphology with a variable aggregate size similar to that reported by Furrer et al. (1992). Because of the low crystallinity of Al_{30} sulfate aged for 72 h (Fig. 1c,d), no definite polygonal morphology could be distinguished for these Keggin cation particles. However, the particles were flake shaped and superimposed on one another, similar to those prepared by Chen et al. (2007) and Motalov et al. (2017) who also confirmed the formation of Al_{30} sulfate under the synthesis protocol used in the present study. On the other hand, the SEM images of the synthesized Al_{13} and Al_{30} associated with the nitrate anions (Fig. 2) revealed that the particle

morphology of Al_{30} nitrate was highly regular and uniformly rectangular with variable aggregate sizes similar to a rhomboid-plate shape (Fig. 2b). The aggregated particles of Al_{13} nitrate had a shape typical of that depicted by Aouad et al. (2006).

Al-Ferron Kinetics Method

The yields for Al_{13} and Al_{30} polycations from the synthesis procedures were examined using the Ferron kinetic method (Jardine and Zelazny 1986; Parker and Bertsch 1992; Zhou et al., 2006). The Ferron kinetics method uses UV-Vis spectroscopy at $\lambda_{\max} = 370$ nm to follow the formation and distribution of the Al species synthesized during the course of the reaction in HPA solution (Fig. 3, Table 1). The percentages of Al species reported by this method were consistent with the

Table 1. Percentage of aluminum species present in Al_{13} and Al_{30} solutions and the rate constant (k)

Sample	Ferron volume (mL)	Sample volume (mL)	Final $[\text{Al}]_{\text{T}}$ (M)	Final $[\text{Ferron}]_{\text{T}}$ (M)	$[\text{Al}_a]$ (%)	$[\text{Al}_b]$ (%)	$[\text{Al}_c]$ (%)	k (min^{-1})
Al_{13}	0.95	0.3	2.4×10^{-5}	1.2×10^{-3}	10.7	74.3	15	0.384
Al_{30}	0.95	0.3	2.4×10^{-5}	1.2×10^{-3}	9.7	14.8	75.5	0.768

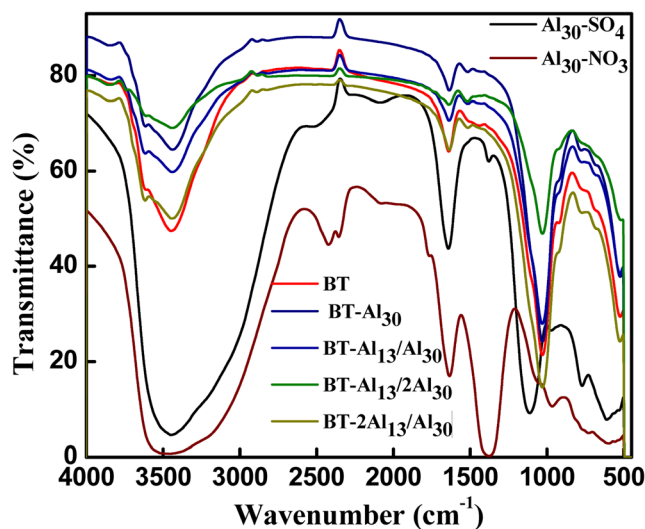


Fig. 4. FTIR spectra for Al_{30} nitrate, Al_{30} sulfate, and BT in addition to the pillared bentonite materials (Al-PILBs)

expected results and revealed Al_{13} and Al_{30} yields of 74.3% and 75.5%, respectively.

FTIR Analysis

The FTIR technique was used to study the structure of polyoxycations precursors and to confirm the successful synthesis of the target Al aggregates and their intercalation inside the BT interlayers (Fig. 4). The aluminum Keggin cations are identified by the AlO_4 group, which is observed as an asymmetrical stretching vibration peak at 769 cm^{-1} . The region between 1200 and 800 cm^{-1} provides information about the structure of BT (Abeysinghe et al. 2013). The weak peak at 1030 cm^{-1} in the spectra of BT, BT- Al_{30} , BT- $\text{Al}_{13}/\text{Al}_{30}$, BT- $\text{Al}_{13}/2\text{Al}_{30}$, and BT- $2\text{Al}_{13}/\text{Al}_{30}$ was assigned to the Si-O stretching vibrations in the aluminosilicate layers of montmorillonite. After intercalation with Al Keggin cations, this peak was replaced by a shoulder, indicating the success of the intercalation. Moreover, the intensity of this shoulder increased

with BT- $2\text{Al}_{13}/\text{Al}_{30}$ and decreased sharply with BT- $\text{Al}_{13}/2\text{Al}_{30}$, suggesting the intercalation of the BT with different Keggin cation ratios. Peaks at 923 and 523 cm^{-1} were associated with Al-OH and Al-O-Si vibrations, respectively. The position of the peak associated with the H-O-H bending vibrations of water molecules adsorbed on BT was shifted from 1639 cm^{-1} to 1635 cm^{-1} in BT- Al_{30} and BT- $2\text{Al}_{13}/\text{Al}_{30}$ materials. The intensity of this peak decreased sharply in the case of BT- $\text{Al}_{13}/2\text{Al}_{30}$. In addition, a strong peak at 3623 cm^{-1} and a broad peak at 3437 cm^{-1} for the BT were assigned to O-H stretching and cation hydration, respectively (Rivera-Jimenez et al. 2011; Abdelkader & Fray 2017). This O-H stretching peak was diminished after intercalation with Keggin cations due to the octahedrally coordinated Al atoms associated with the hydroxyl group of the Al polycations, especially for BT- $\text{Al}_{13}/2\text{Al}_{30}$ material. In conclusion, variations in positions and intensity for those peaks are probably attributable to intercalation with differing types and ratios of Keggin cations.

Table 2. Chemical analysis (wt.%) of the energy-dispersive X-ray (EDX) for Al Keggin cations and Al-PILBs materials

Element	$\text{Al}_{30}\text{-SO}_4$	$\text{Al}_{13}\text{-SO}_4$	BT	BT- Al_{30}	BT- $\text{Al}_{13}/\text{Al}_{30}$	BT- $\text{Al}_{13}/2\text{Al}_{30}$	BT- $2\text{Al}_{13}/\text{Al}_{30}$
Sodium (Na)			4.53	1.01	1.44	1.76	1.74
Calcium (Ca)			2.61	1.86	2.04	1.73	2.06
Silicon (Si)			50.31	50.43	50.08	54.58	50.39
Aluminum (Al)	60.35	62.91	16.57	19.85	20.83	20.44	20.58
Magnesium (Mg)			3.45	3.02	3.03	3.15	3.50
Potassium (K)			3.13	2.41	3.16	1.73	2.80
Iron (Fe)			14.68	15.24	14.54	10.52	14.24
Titanium (Ti)			2.64	3.68	3.19	3.48	2.79
Vanadium (V)			0.76	0.67	0.41	0.71	0.42
Sulfur (S)	39.65	37.09	1.11	1.03	1.29	1.26	1.48

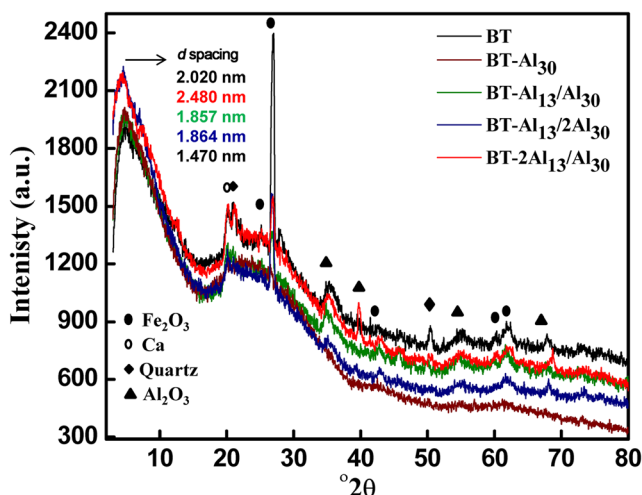


Fig. 5. XRD patterns for BT and Al-PILBs. Inset are the data from XRD analysis and basal spacing and changes in them in comparison to the raw BT basal spacing

Energy Dispersive X-ray Analysis

Analysis by EDX showed an increase in the Al content of Al-PILB materials relative to BT showing that Al polyoxycations of Al_{13} and Al_{30} were incorporated into the interlayer nanospaces. Moreover, Na content decreased in all Al-PILB materials because of the cation exchange between Na and Al Keggin cations. In most materials, both Ca and Mg exhibited a moderate decrease, indicating the low probability of participating in the intercalation process (Table 2). Finally, the Si/Al ratios in Al-PILBs materials decreased, confirming the success of the intercalation process.

X-ray Diffraction Analysis

The results of XRD analysis (Fig. 5) showed an increase in basal spacing, d_{001} , for all Al-PILB materials by varying degrees relative to raw BT, $d_{001} = 1.53$ nm (El Bouraie and Masoud 2017). The decrease in basal spacing in BT (to 1.47 nm) was due to dehydration of the interlayer and, therefore, the collapse of layers by ~ 0.06 nm after calcination at 300°C for 3 h. The intense, sharp quartz peak confirmed quartz as the major impurity in BT. The difference in sharpness and intensity in Al-PILBs peaks is probably attributable to the presence of polyoxycations in various ratios within the BT interlayers, regardless of the type of Al Keggin cation (Sanabria et al. 2008). The broadness of the peaks may be explained by the small number of stacked pillared layers that could have occurred because of slow replacement of the exchangeable Na cations by the larger Al_{13} and/or Al_{30} aggregates.

Texture Analysis of the Al-PILB Materials Synthesized

Intercalation processes are known to create more pores, gaps, and several other types of defects in host materials. To investigate the effect of the intercalation on the porosity of BT, N_2 adsorption/desorption measurements were used to calculate specific surface area (S_A), pore diameter (D_p), and pore volume (Fig. 6). The isotherms obtained were of the

common type II of Brunauer's classification, as observed typically in multilayer materials. The hysteresis loops of Al-PILB materials belonged to type H4 (IUPAC classification); and most of the hysteresis loops were closed at low relative pressures, indicating the presence of micropores (Farrag 2016). From this approach, the synthesized Al-PILB materials showed the advantages of having a large surface area and large pore size after pillaring with Al polyoxycations, compared to the pristine BT (Table 3). The large pore size observed for BT- Al_{30} (2.59 nm) and BT- $\text{Al}_{13}/2\text{Al}_{30}$ (2.48 nm) compared to BT- $\text{Al}_{30}/\text{Al}_{13}$ (2.13 nm) and BT- $\text{Al}_{30}/2\text{Al}_{13}$ (2.13 nm) was probably due to large proportions of the bulky Al_{30} being intercalated inside BT interlayers. This induced differing physical morphologies for the synthesized compounds, which led to noticeable changes in their pore sizes. This interpretation coincides with XRD results which showed that the Al-PILBs peaks shifted to lower 2θ (i.e. increased in basal spacing).

Pesticides Adsorption Assays

The behavior of a mixture of chlorinated pesticides on adsorption into the synthesized Al-PILBs was investigated under optimal ion-adsorption conditions (natural pH, Al-PILBs weight 25 mg, solution volume 25 mL, and 25°C) (Fig. 7). Adsorption capacities of the heptachlor epoxide, dieldrin, endrin, endosulfan 1, and endosulfan 2 into BT- Al_{30} and BT- $\text{Al}_{13}/2\text{Al}_{30}$ were the largest among the other pesticides studied (Table 4). Both BT- Al_{30} and BT- $\text{Al}_{13}/2\text{Al}_{30}$ adsorbed dieldrin to almost the same extent. The data showed a significant adsorption capability for the pillared BT containing high proportions of Al_{30} polyoxycations (i.e. BT- Al_{30} and BT- $\text{Al}_{13}/2\text{Al}_{30}$). This may be attributed to the porous characteristic represented by the large surface area and suitable pore size (21.3–25.9 Å) of synthesized Al-PILBs containing Al_{30} polyoxycations. The adsorption behavior of the target pesticides, therefore, was influenced by the size and charge of Al polyoxycations in the interlayer spaces.

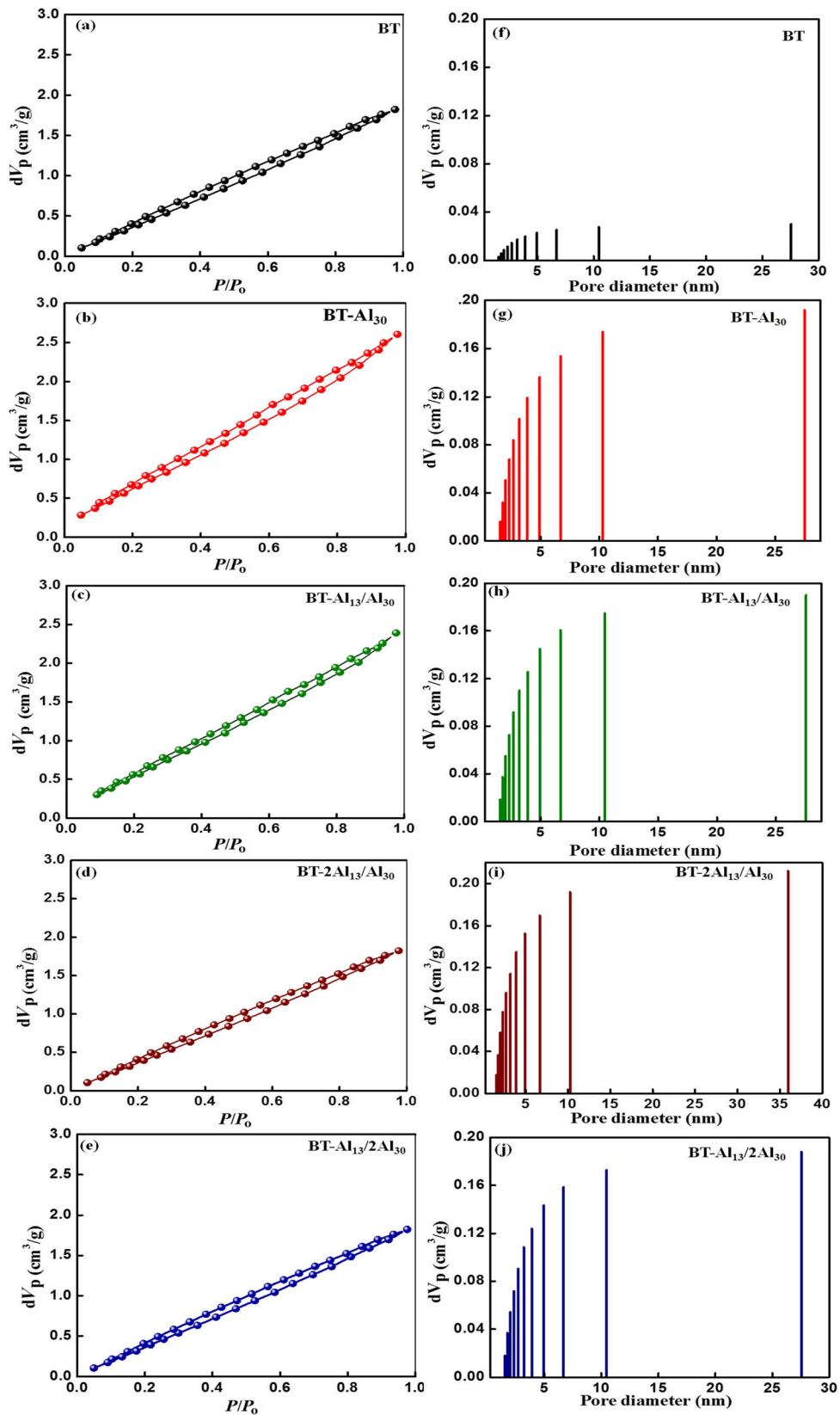


Fig. 6. Nitrogen adsorption/desorption isotherms for BT and the synthesized Al-PILBs

Table 3. Textural characteristics of the Al-PILBs from N₂ adsorption/desorption measurements

Sample	S_A (m ² /g)	ES_A (m ² /g)	PS_A (m ² /g)	Total pore volume (cc/g)	Micropore volume (cc/g)	Mesopore volume (cc/g)	D_p (nm)
BT	29	20	9	0.092	0.001	0.0910	0.62
BT-Al ₃₀	163	130	33	0.212	0.013	0.199	2.59
BT-Al ₁₃ /Al ₃₀	189	131	58	0.202	0.006	0.196	2.13
BT-Al ₁₃ /2Al ₃₀	187	138	48	0.232	0.016	0.216	2.48
BT-2Al ₁₃ /Al ₃₀	184	127	57	0.196	0.006	0.190	2.13

* S_A , ES_A , PS_A , and D_p denoted for specific surface area, external surface area, pores surface area, and average pore size, respectively.

The adsorption of these non-ionic organochlorine pesticides into pillared clays is explained by the combination of hydrophobic interaction and by hydrogen bonding between hydroxyl groups of polycations and oxygen in the pesticide structure. The adsorption efficiency of the Al-PILB materials toward heptachlor epoxide, dieldrin, and endrin may be ascribed to the strong binding affinity of the epoxide group (CH₂)₂O (Rinaldi & Kristiani, 2017). BT has a negatively charged surface in addition to the Lewis acidic character of the intercalated Al₃₀ polycation. The pesticide molecules thus adsorbed firmly on the Al-PILB surface through the negatively charged oxygen of Al₃₀ polycations and the positively charged carbon centers in the pesticide molecules BT surfaces (Rinaldi and Kristiani 2017). The strong binding is probably due, therefore, to the epoxide group in which the BT-Al₃₀ catalyzed the ring-opening of epoxides using water as the reaction medium (Bonollo et al. 2011) (Table 4).

The effect of the initial concentration of three selected pesticides (heptachlor epoxide, dieldrin, and endrin) (Table 5) on uptake by BT-Al₃₀ material was investigated within the concentration range 2.5–200 µg/L under the optimum experimental conditions (natural pH, BT-Al₃₀ weight 25 mg, solution volume 25 mL, and 25°C). The adsorption capacities of heptachlor epoxide, dieldrin, and endrin onto BT-Al₃₀ at optimum pH were 59.2, 59.15, and 60 µg/g, compared with 34.68, 39.45, and 38.9 for the pristine BT, respectively (Fig. 8). The uptake of target pesticides increased sharply as the concentration increased. Moreover, the removal efficiency of heptachlor epoxide, dieldrin, and endrin was reduced from 81.2% and 81% to 70% and 60%, respectively, when the Al₃₀/Al₁₃ ratio was decreased in Al-PILBs. These findings showed good binding interactions of the pesticides to the surface of Al-PILBs under optimal conditions. The adsorption data were plotted using several isotherm models such as Langmuir,

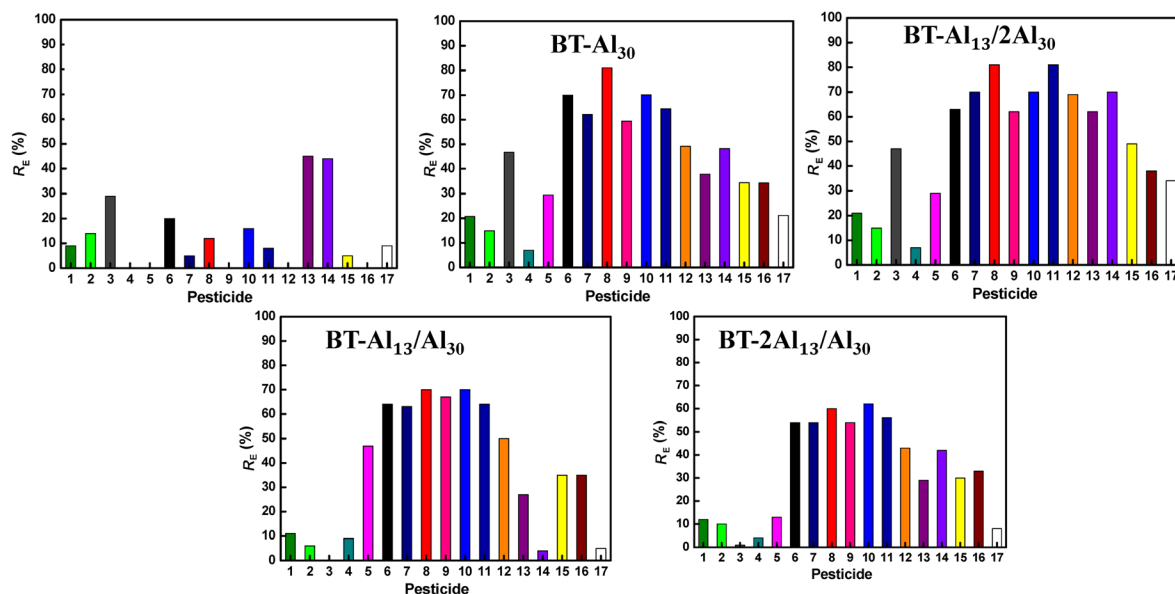


Fig. 7. The detailed adsorption profiles of Al-PILBs for 17 pesticides at selected optimal conditions (e.g. time 5 h, pH 5.8 (natural pH), and 25°C). The mixture of pesticides included the following: (1) α -BHC, (2) β -BHC, (3) σ -BHC, (4) heptachlor, (5) aldrin, (6) heptachlor epoxide, (7) endosulfan 1, (8) dieldrin, (9) DDE, (10) endrin, (11) endosulfan 2, (12) DDD, (13) endrin (14) endosulfan sulfate, (15) DDT, (16) methoxychlor, and (17) γ -BHC

Table 4. Comparisons among various adsorbents used for pesticide removal from polluted water

Adsorbent	Removal (%)	Pesticide	References
Zeolites	25.8–92.1	Bentazon, clopyralid	(Valičková et al. 2013; De Smedt et al. 2015)
Zeolites/surfactant	>94	Carbamate	(Arnok and Burakham 2014)
AC/Fe ⁰	>70	Atrazine	(Morales-Pérez et al. 2015)
Cyclodextrines	>92	DDE, DDD, DD	(Zolfaghari 2016)
NH ₄ Cl-AC	97.5	Diazion	(Moussavi et al. 2013)
Activated carbon	90–100	Bromopropylate	(Ioannidou et al. 2010)
Bentonite/quaternary ammonium	81.5, 91.5	Butachlor, malathion	(Pal and Vanjara 2001)
GO and RGO	100	Endosulfan, chlorpyrifos, malathion	(Maliyekkal et al. 2013)
Silica/PANI	97	Chloridazon	(El-Said et al. 2018)
Al-PILBs	>98	Heptachlor epoxide, dieldrin, endrin	(This work)

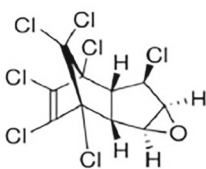
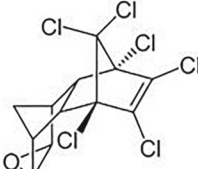
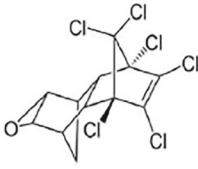
Freundlich, and Sips, but only the Freundlich model fitted well with the adsorption data for heptachlor epoxide, dieldrin, and endrin onto BT-Al₃₀, with correlation coefficients (R^2) >0.96 for the target pesticides (Fig. 8). Freundlich (1906) used a multi-site adsorption assumption and his isotherm model is given by Eq. (3).

$$q_e = K_f C_e^{1/n} \quad (3)$$

The Freundlich adsorption coefficient (K_f , L^{1/n} mg^(1-1/n)/g) describes the adsorption capacity of the target pesticides onto BT-Al₃₀ micropores at equilibrium concentration and $1/n$ (dimensionless) reflects the degree to which adsorption is a function of concentration. The values of $1/n < 1$ obtained from adsorption of heptachlor epoxide, dieldrin, and endrin on BT-Al₃₀ indicate that adsorption follows the L-type isotherm (Giles et al. 1960). This means that competition for adsorption sites became greater as the concentration increased. The extent of adsorption of the endrin and dieldrin on BT-Al₃₀ at a solution concentration of 20 µg/L was similar (60 and 59.2 µg/g, respectively); whereas heptachlor epoxide reached that

same level (59.15 µg/g) at a solution concentration of 16 µg/L, indicating that its adsorption could be greater than the other two. The octanol/water partition coefficient (K_{ow}) is well known as a measure of the hydrophobicity of the pesticide and may predict the relative efficiency of pesticide removal. The values for log K_{ow} of the target pesticides followed the order heptachlor epoxide > endrin > dieldrin (Table 5). The greater the log K_{ow} value, the more hydrophobic the compound; therefore, heptachlor epoxide is the most likely of the three to adsorb into BT-Al₃₀ pores at a low initial concentration (Gupta et al. 2011). The removal efficiencies of heptachlor epoxide, dieldrin, and endrin using 10, 15, and 25 mg of BT-Al₃₀ material were 40, 65, and 99%, respectively. However, the adsorption efficiency varied slightly at a dose >25 mg; giving values >99%. In Table 6, the adsorption behavior of various pillared clays for the various organic compounds, including the pesticides, is summarized. When pesticides were desorbed using acetone; ~67.5% of the loaded pesticides were released from the BT-Al₃₀. These results indicated that the BT-Al₃₀ is a potential candidate for the reproducible removal of chlorinated pesticides from water in the environment.

Table 5. The chemical structure and physico-chemical properties of the most selective pesticides for the synthesized Al-PILB materials

	¹ Heptachlor epoxide	² Endrin	³ Dieldrin
Formula	C ₁₀ H ₅ Cl ₇ O	C ₁₂ H ₈ Cl ₆ O	C ₁₂ H ₈ Cl ₆ O
Structure Formula			
Molar Weight (g/mol)	389.3	380.91	380.91
Density (g/cm ³)	1.58	1.64	1.75
Water solubility (µg/L)	350	230	186
log K_{ow}	5.40	4.56	4.54

¹ WHO (2004); ² IPCS (1992); ³ WHO (1989)

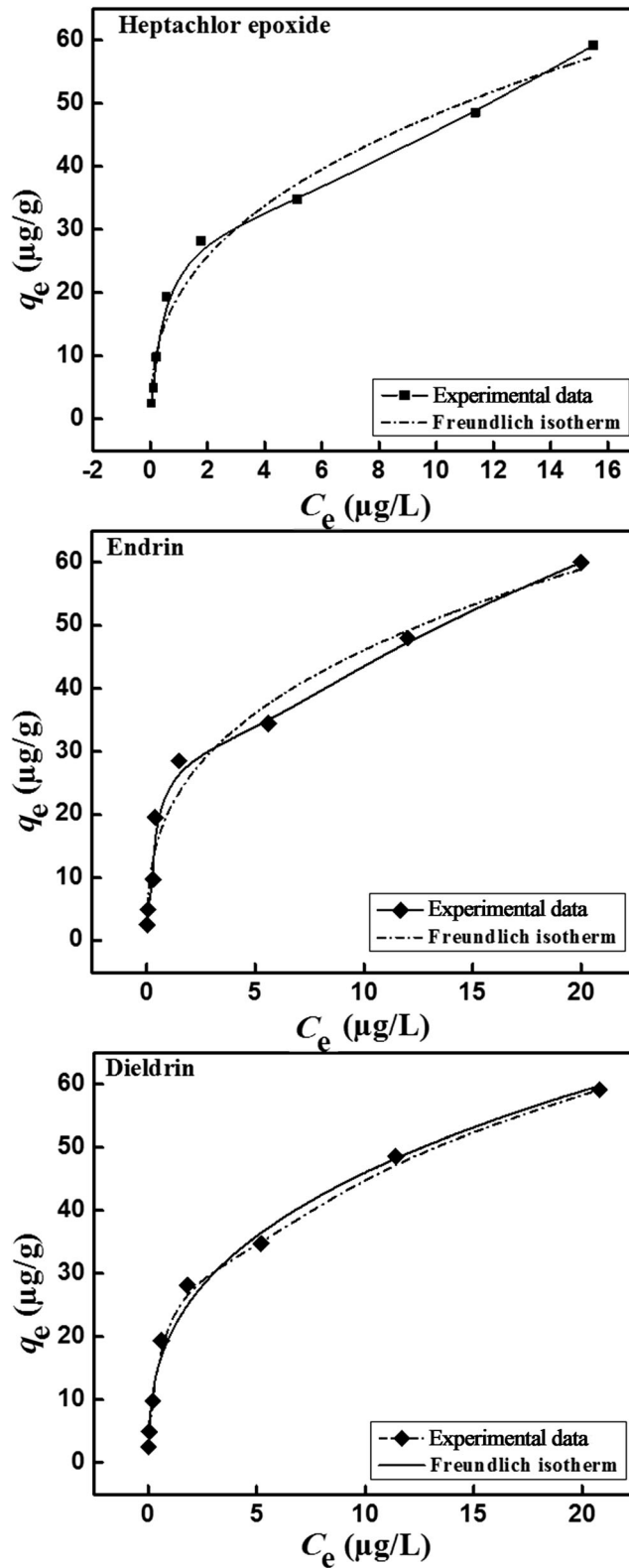


Fig. 8. Experimental isotherms (symbols) and Freundlich isotherms (dash) for the equilibrium adsorption of heptachlor epoxide, dieldrin, and endrin onto BT- Al_{30} from a single ion solution; equilibrium time 5 h, pH 5.8, and 25°C

Table 6. Behaviors of various clay pillars on the adsorption of organic molecules from aqueous solution

Pillar type	Organic adsorbate	Adsorption behavior	References
HAl-MX80	3-chloroaniline(3-CA) and atrazine (AT)	100–90% 3-CA and 53–24% AT ($C_i = 2.0\text{--}9.7\ \mu\text{M}$, 3-CA and $0.25\text{--}7.5\ \mu\text{M}$, AT) at pH 5.7	(Matthes and Kahr 2000)
HZr-MX80	3-chloroaniline(3-CA) and atrazine (AT)	100–99% 3-CA and 43–28% AT ($C_i = 2.0\text{--}9.7\ \mu\text{M}$ (pH 5.4) 3-CA and $0.25\text{--}7.5\ \mu\text{M}$ (pH 5.6), AT)	(Matthes et al. 2000)
CTA-TixHy-montm CTA-Alx (OH)y-montm CTAFex (OH)y-montm	Diuron	3500–3700 $\mu\text{g/L}$ at pH 3.1 ($C_i = 5\ \text{mg/L}$) Ti>Fe>Al	(Bouras et al. 2007)
Al-PILC	Thiabendazol	11.78 – 17.50 mg/g at pH 6 ($C_i = 2\text{--}100\ \text{mg/L}$)	(Jalil et al. 2014)
Al-PILC	Thiabendazol	63.87 mg/g (pH 6)	(Jalil et al. 2013)
MAIOr-NaBt (M = Ni, Cu, Co)	Bisphenol A (BPA) and 2,4-dichlorophenol (DCP)	5 and 3 mg/g for BPA and DCP, respectively (neutral pH)	(Ortiz-Martínez et al. 2016)
Alumina-pillared montmorillonite (AIPMt)	2,4-dichlorophenol, 2,4,6-trichlorophenol and pentachlorophenol	26.3% of 2,4-dichlorophenol, 75.6% of 2,4,6-trichlorophenol and 95.2% of pentachlorophenol	(Danis et al. 1998)
TOMA-Montmorillonite	Atrazine	64.7–74.6%	(Dutta and Singh 2015)
BT- Al_{30}	Heptachlor epoxide, dieldrin, endrin	>98	(This work)

CONCLUSIONS

In this study, the synthesis of Al-PILBs containing various ratios of Al_{13} and Al_{30} Keggin cations was carried out through the concentration method using the nitrate form to create Al pillars. The chemical and textural characteristics of the synthesized Al-PILBs were investigated using XRD, SEM, EDX, FTIR, UV-Vis spectroscopy, and N_2 adsorption-desorption measurements. The maximum adsorption of heptachlor epoxide, dieldrin, and endrin pesticides onto BT- Al_{30} at natural pH was 59.2, 59.15, and 60 $\mu\text{g/g}$, respectively, at equilibrium solution concentrations of 16, 20, and 20 $\mu\text{g/L}$, respectively. The adsorption experimental results were fitted to the Freundlich model. The significant adsorption efficiency of BT- Al_{30} , which is related to the negatively charged surface of BT in addition to the intercalation with Al_{30} polycations, means that the bentonite is useful for remediating pesticide-contaminated water.

Compliance with Ethical Standards

Conflict of Interests

The authors declare no conflict of interests.

REFERENCES

- Abdelkader, A. M., & Fray, D. J. (2017). Controlled electrochemical doping of graphene-based 3D nanoarchitecture electrodes for supercapacitors and capacitive deionisation. *Nanoscale*, 9, 14548–14557.
- Abdelkader, A. M., Patten, H. V., Li, Z., Chen, Y., & Kinloch, I. A. (2015). Electrochemical exfoliation of graphite in quaternary ammonium-based deep eutectic solvents: a route for the mass production of graphene. *Nanoscale*, 7, 11386–11392.
- Abeysinghe, S., Unruh, D. K., & Forbes, T. Z. (2013). Surface modification of Al_{30} Keggin-type polyaluminum molecular clusters. *Inorganic Chemistry*, 52, 5991–5999.
- Aouad, A., Mandalia, T., & Bergaya, F. (2005). A novel method of Al-pillared montmorillonite preparation for potential industrial up-scaling. *Applied Clay Science*, 28, 175–182.
- Aouad, A., Pineau, A., Tchoubar, D., & Bergaya, F. (2006). Al-pillared montmorillonite obtained in concentrated media. Effect of the anions (nitrate, sulfate and chloride) associated with the Al species. *Clays and Clay Minerals*, 54, 626–637.
- Annok, P., & Burakham, R. (2014). Retention of carbamate pesticides by different surfactant-modified sorbents: a comparative study. *Journal of the Brazilian Chemical Society*, 25, 1720–1729.
- Aznárez, A., Delaigle, R., Eloy, P., Gaigneaux, E. M., Korili, S. A., & Gil, A. (2015). Catalysts based on pillared clays for the oxidation of chlorobenzene. *Catalysis Today*, 246, 15–27.
- Barrer, R. (1986). Expanded clay minerals: A major class of molecular sieves. *Journal of Inclusion Phenomena*, 4, 109–119.
- Bonilla-Petriciolet, A., Mendoza-Castillo, D. I., & Reynel-Ávila, H. E. (2017). *Adsorption Processes for Water Treatment and Purification*. Berlin, Germany: Springer International Publishing.
- Bonollo, S., Lanari, D., & Vaccaro, L. (2011). Ring-Opening of Epoxides in Water. *European Journal of Organic Chemistry*, 2011, 2587–2598.
- Bouras, O., Bollinger, J.-C., Baudu, M., & Khalaf, H. (2007). Adsorption of diuron and its degradation products from aqueous solution by surfactant-modified pillared clays. *Applied Clay Science*, 37, 240–250.
- Cheira, M., Mira, H., Sakr, A., & Mohamed, S. (2019). Adsorption of U (VI) from acid solution on a low-cost sorbent: equilibrium, kinetic, and thermodynamic assessments. *Nuclear Science and Techniques*, 30(2019), 156.
- Chen, Z., Luan, Z., Fan, J., Zhang, Z., Peng, X., & Fan, B. (2007). Effect of thermal treatment on the formation and transformation of Keggin Al_{13} and Al_{30} species in hydrolytic polymeric aluminum solutions. *Colloids and Surfaces A: Physicochemical and Engineering Aspects*, 292, 110–118.
- Cool P. & Vansant E.F. (1998). Pillared clays: Preparation, characterization and applications. Pp. 265–288 in: *Synthesis. Molecular Sieves Science and Technology*, vol 1 (H.G. Karge and J. Weitkamp, editors). Springer, Berlin, Heidelberg.

- Danis, T. G., Albanis, T. A., Petrakis, D. E., & Pomonis, P. J. (1998). Removal of chlorinated phenols from aqueous solutions by adsorption on alumina pillared clays and mesoporous alumina aluminum phosphates. *Water Research*, *32*, 295–302.
- De Smedt, C., Ferrer, F., Leus, K., & Spanoghe, P. (2015). Removal of pesticides from aqueous solutions by adsorption on zeolites as solid adsorbents. *Adsorption Science and Technology*, *33*, 457–485.
- De Wilde, T., Mertens, J., Simunek, J., Sniegowski, K., Ryckeboer, J., Jaeken, P., Springael, D., & Spanoghe, P. (2009). Characterizing pesticide sorption and degradation in microscale biopurification systems using column displacement experiments. *Environmental Pollution*, *157*, 463–473.
- Del Riego, A., Herrero, I., Pesquera, C., Blanco, C., Benito, I., & González, F. (1994). Preparation of PILC-Al through dialysis bags: a comparative study. *Applied Clay Science*, *9*, 189–197.
- Dutta, A., & Singh, N. (2015). Surfactant-modified bentonite clays: preparation, characterization, and atrazine removal. *Environmental Science and Pollution Research*, *22*, 3876–3885.
- El Bouraie, M., & Masoud, A. A. (2017). Adsorption of phosphate ions from aqueous solution by modified bentonite with magnesium hydroxide Mg(OH)₂. *Applied Clay Science*, *140*, 157–164.
- El-Said, W., El-Khouly, M., Ali, M., Rashad, R., Al-Bogami, A., Elshehy, E. A., & Al-Bogami, A. (2018). Synthesis of mesoporous silica-polymer composite for the chloridazon pesticide removal from aqueous media. *Journal of Environmental Chemical Engineering*, *6*, 2214–2221.
- Farrag, M. (2016). Enantioselective silver nanoclusters: Preparation, characterization and photoluminescence spectroscopy. *Materials Chemistry and Physics*, *180*, 349–356.
- Freundlich, H. M. F. (1906). Über die adsorption in losungen. *Zeitschrift für Physikalische Chemie*, *57*, 387–470.
- Furrer, G., Ludwig, C., & Schindler, P. W. (1992). On the chemistry of the Keggin Al₁₃ polymer: I Acid-base properties. *Journal of Colloid and Interface Science*, *149*, 56–67.
- Giles, C. H., Macewan, T. H., Nakhwa, S. N., & Smith, D. (1960). Studies in adsorption. part XI. A system of classification of solution adsorption isotherms, and its use in diagnosis of adsorption mechanisms and in measurement of specific surface areas of solids. *Journal of the Chemical Society*, *14*, 3979–3993.
- Gupta, V. K., Gupta, B., Rastogi, A., Agarwal, S., & Nayak, A. (2011). Pesticides removal from waste water by activated carbon prepared from waste rubber tire. *Water Research*, *149*, 4047–4055.
- Hamza, M., Weie, Y., Mira, H., Abdel-Rahman, A., & Guibal, E. (2019). Synthesis and adsorption characteristics of grafted hydrazinyl amine magnetite-chitosan for Ni (II) and Pb (II) recovery. *Chemical Engineering Journal*, *362*, 310–324.
- Hladik, M. L., Roberts, A. L., & Bouwer, E. J. (2005). Removal of neutral chloroacetamide herbicide degradates during simulated unit processes for drinking water treatment. *Water Research*, *39*, 5033–5044.
- Ioannidou, O. A., Zabanitou, A. A., Stavropoulos, G. G., Md, I., & Albanis, T. A. (2010). Preparation of activated carbons from agricultural residues for pesticide adsorption. *Chemosphere*, *80*, 1328–1336.
- IPCS (1992). *Endrin*. Geneva, World Health Organization, International Programme on Chemical Safety (Environmental Health Criteria 130).
- Jalil, M. E., Baschini, M., Rodríguez-Castellón, E., Infantes-Molina, A., & Sapag, K. (2014). Effect of the Al/clay ratio on the thiabendazole removal by aluminum pillared clays. *Applied Clay Science*, *87*, 245–253.
- Jalil, M. E., Vieira, R. S., Azevedo, D., Baschini, M., & Sapag, K. (2013). Improvement in the adsorption of thiabendazole by using aluminum pillared clays. *Applied Clay Science*, *71*, 55–63.
- Jardine, P., & Zelazny, L. (1986). Mononuclear and polynuclear aluminum speciation through differential kinetic reactions with ferron. *Soil Science Society of America Journal*, *50*, 895–900.
- Kumararaja, P., Manjaiah, K. M., Datta, S. C., & Sarkar, B. (2017). Remediation of metal contaminated soil by aluminium pillared bentonite: Synthesis, characterisation, equilibrium study and plant growth experiment. *Applied Clay Science*, *137*, 115–122.
- Lin, J.-L., Chin, C.-J., Huang, C., Pan, J. R., & Wang, D. (2008). Coagulation behavior of Al₁₃ aggregates. *Water Research*, *42*, 4281–4290.
- Mallyekkal, S. M., Sreepasad, T. S., Krishnan, D., Kouser, S., Mishra, A. K., Waghmare, U. V., & Pradeep, T. (2013). Graphene: A reusable substrate for unprecedented adsorption of pesticides. *Small*, *9*, 273–283.
- Matthes, W., & Kahr, G. (2000). Sorption of organic compounds by Al and Zr-hydroxy-intercalated and pillared bentonite. *Clays and Clay Minerals*, *48*, 593–602.
- Ming-li, C., Yong-fu, Y., Ji-zu, Y., & Ming-he, C. (2002). Preparation and properties of pillared montmorillonite by polyhydroxyl-aluminum-manganese cations. *Journal of Wuhan University of Technology-Mater. Sci. Ed*, *17*, 43–46.
- Morales-Pérez, A. A., Arias, C., & Ramírez-Zamora, R. M. (2015). Removal of atrazine from water using an iron photo catalyst supported on activated carbon. *Adsorption*, *22*, 49–58.
- Motalov, V., Karasev, N. S., Ovchinnikov, N. L., & Butman, M. F. (2017, 2017). Thermal emission of alkali metal ions from Al₃₀-pillared montmorillonite studied by mass spectrometric method. *Journal of Analytical Methods in Chemistry*, 2090–8865. <https://doi.org/10.1155/2017/4984151>
- Moussavi, G., Hosseini, H., & Alahabadi, A. (2013). The investigation of diazinon pesticide removal from contaminated water by adsorption onto NH₄Cl-induced activated carbon. *Chemical Engineering Journal*, *214*, 172–179.
- Okada, T., Seki, Y., & Ogawa, M. (2014). Designed nanostructures of clay for controlled adsorption of organic compounds. *Journal of Nanoscience and Nanotechnology*, *14*, 2121–2134.
- Ortiz-Martínez, K., Reddy, P., Cabrera-Lafaurie, W. A., Román, F. R., & Hernández-Maldonado, A. J. (2016). Single and multi-component adsorptive removal of bisphenol A and 2,4-dichlorophenol from aqueous solutions with transition metal modified inorganic-organic pillared clay composites: Effect of pH and presence of humic acid. *Journal of Hazardous Materials*, *312*, 262–271.
- Pal, O. R., & Vanjara, A. K. (2001). Removal of malathion and butachlor from aqueous solution by clays and organoclays. *Separation and Purification Technology*, *24*, 167–172.
- Parker, D. R., & Bertsch, P. M. (1992). Identification and quantification of the "Al₁₃" tridecameric aluminum polycation using ferron. *Environmental Science and Technology*, *26*, 908–914.
- Rinaldi, N., & Kristiani, A. (2017). Physicochemical of pillared clays prepared by several metal oxides. *AIP Conf. Proceedings 2017(1823)*, 020063.
- Rivera-Jimenez, S. M., Lehner, M., Cabrera-Lafaurie, W. A., & Hernández-Maldonado, A. J. (2011). Removal of naproxen, salicylic acid, clofibrac acid, and carbamazepine by water phase adsorption onto inorganic-organic-intercalated bentonites modified with transition metal cations. *Environmental Engineering Science*, *28*, 171–182.
- Rowell, J., & Nazar, L. (2000). Speciation and thermal transformation in alumina sols: Structures of the polyhydroxyoxoaluminum cluster [Al₃₀O₈(OH)₅₆(H₂O)₂₆]³⁸⁺ and its δ-Keggin moiety. *Journal of the American Chemical Society*, *122*, 3777–3778.
- Sanabria, N., Alvarez, A., Molina, R., & Moreno, S. (2008). Synthesis of pillared bentonite starting from the Al-Fe polymeric precursor in solid state, and its catalytic evaluation in the phenol oxidation reaction. *Catalysis Today*, *133–135*, 530–533.
- Şans, B. E., Güven, O., Esenli, F., & Çelik, M. S. (2017). Contribution of cations and layer charges in the smectite structure on zeta potential of Ca-bentonites. *Applied Clay Science*, *143*, 415–421.
- Schoonheydt, R. A., & Leeman, H. (1992). Pillaring of saponite in concentrated medium. *Clay Minerals*, *27*, 249–252.
- Schoonheydt, R. A., Leeman, H., Scorpion, A., Lenotte, I., & Grobet, P. (1994). The Al pillaring of clays. Part II. Pillaring with [Al₁₃O₄(OH)₂₄(H₂O)₂]⁷⁺. *Clays and Clay Minerals*, *42*, 518–525.
- Valičková, M., Derco, J., & Šimovičová, K. (2013). Removal of selected pesticides by adsorption. *Acta Chimica Slovaca*, *6*, 25–28.

- Vicente, M. A., & Lambert, J. F. (2003). Al-pillaring of saponite with the Al polycation $[Al_{13}(OH)_{24}(H_2O)_{24}]^{13+}$ using a new synthetic route. *Clays and Clay Minerals*, 51, 168–171.
- Wang, M., & Muhammed, M. (1999). Novel Synthesis of Al_{13} -cluster based alumina materials. *Nanostructured Materials*, 11, 1219–1229.
- WHO (1989). Aldrin and dieldrin. Geneva, World Health Organization, International Programme on Chemical Safety (Environmental Health Criteria 91).
- WHO (2004). Heptachlor and heptachlor epoxide in drinking-water. Geneva, Switzerland, World Health Organization, background document for development of WHO Guidelines for drinking-water quality.
- Yuan, P., Xiaolin, Y., He, H., Dan, Y., Linjiang, W., & Jianxi, Z. (2006). Investigation on the delaminated-pillared structure of TiO_2 -PILC synthesized by $TiCl_4$ hydrolysis method. *Microporous and Mesoporous Materials*, 93, 240–247.
- Zhou, W., Gao, B., Yue, O., Liu, L., & Wang, Y. (2006). Al-Ferron kinetics and quantitative calculation of Al (III) species in polyaluminum chloride coagulants. *Colloids and Surfaces, A: Physicochemical and Engineering Aspects*, 278, 235–240.
- Zhu, J., Wen, K., Zhang, P., Wang, Y., Ma, L., Xi, Y., Zhu, R., Liu, H., & He, H. (2017). Keggin- Al_{30} pillared montmorillonite. *Microporous and Mesoporous Materials*, 242, 256–263.
- Zolfaghari, G. (2016). β -Cyclodextrin incorporated nanoporous carbon: host-guest inclusion for removal of p-Nitrophenol and pesticides from aqueous solutions. *Chemical Engineering Journal*, 283, 1424–1434.

(Received 20 July 2019; revised 9 March 2020; Accepted 18 March 2020; AE: Yuji Arai)